DFT+U-type functional derived to explicitly address the flat plane condition

Andrew C. Burgess [1] Edward Linscott [2] and David D. O'Regan [1,*]

^{1}*School of Physics, Trinity College Dublin, The University of Dublin, Ireland*
^{2}*Theory and Simulation of Materials (THEOS), Faculté des Sciences et Techniques de l'Ingénieur,*
École Polytechnique Fédérale de Lausanne, CH-1015 Lausanne, Switzerland

A DFT+U-type corrective functional is derived from first principles to enforce the flat plane condition on localized subspaces, thus dispensing with the need for an ad hoc derivation from the Hubbard model. Small, molecular test systems at the dissociated limit are used to compare the functional form against several previously proposed DFT+U-type functionals. The functional derived here yields relative errors below 0.6% in the total energy of the dissociated s-block dimers as well as the dissociated H_5^+ ring system, a challenging test case in which the asymmetric, tilted flat plane condition applies. In comparison, bare PBE and PBE+U (using Dudarev's 1998 Hubbard functional) yields relative energetic errors as high as 8.0% and 20.5%, respectively.

Since the inception of the Hohenberg-Kohn theorems [1], practitioners of density functional theory (DFT) have sought more accurate, reliable, and efficient density functional approximations (DFAs) to the exchange correlation functional E_{xc}^{approx} [2–13]. Despite these DFAs' remarkable success in predicting mechanical properties [14] and crystallographic structures [15], they still exhibit significant failures in the prediction of molecular bond dissociation [16–18], band gaps in solids [19–21], and polymorph energy differences in transition metal oxides [22–24]. Many of these failures can be attributed to the breaking of certain exact physical constraints, namely (i) the piecewise linearity condition with respect to electron count [25] and (ii) the constancy condition with respect to magnetization [26,27]. The breaking of these two exact conditions is referred to as many-electron self-interaction error (MSIE) [16,28] and static correlation error (SCE) [27,29], respectively. The generalization of these two conditions is referred to as the "flat plane condition" [30].

For a two-electron system it is known that the total energy with respect to electron count and magnetization $E_{tot}[N_{tot}, M_{tot}]$ will typically be composed of two flat planes which meet with a derivative discontinuity along the $N_{tot} = 1$ line. This is referred to as a "Type 1" flat plane [31] and it will occur when the convexity condition is met

$$2E_{tot}[N_{tot}] < E_{tot}[N_{tot} + 1] + E_{tot}[N_{tot} - 1], \quad (1)$$

for $N_{tot} = 1$. This particular two-electron flat plane structure will be referred to as the "diamond" for brevity. An equivalent flat plane will also form for the individual components of the total energy such as the Hartree-exchange-correlation energy E_{Hxc}, as shown by Ayers, Cuevas-Saavedra *et al.* [32,33]. Total electronic energies for systems with certain integer numbers of spin-up and spin-down electrons are well approximated by currently available DFAs. However, large deviations from the

exact total energies were reported for systems with noninteger values, as shown in Fig. 1.

There are similar conditions for many-atom systems. For a system of N_{atom} isolated atomic sites with a total of N_{tot} electrons, a piecewise linearity condition with respect to electron count should occur separately at each atomic site where $N_{atom}, N_{tot} \in \mathbb{N}$ but $N_{tot}/N_{atom} \notin \mathbb{N}$. To see this, let us temporarily define $N = \lfloor N_{tot}/N_{atom} \rfloor$, where $\lfloor \cdot \rfloor$ is the floor function (the integer part). Then, the total energy of the system with N_{tot}/N_{atom} electrons at each atomic site should be equal in energy to the system with k sites with $N + 1$ electrons and $N_{atom} - k$ sites with N electrons, where $k < N_{atom}$ and $N_{tot} = NN_{atom} + k$. However, current DFAs yield incorrect energies for systems with fractional occupancies at the atomic sites [34]. We refer to this error as "local-MSIE" as, in this case, one varies the local occupancy at the atomic site N, as opposed to the global electron count N_{tot} [35]. Analogously, there exists local-SCE and a local analog of the flat plane condition. Local-MSIE and local-SCE will lead to erroneous total energies even for systems with integer global electron counts N_{tot}.

Assuming local-MSIE is predominantly quadratic in nature (as was reported for global-MSIE [36]), the local-MSIE at an atomic site can be alleviated with an energetic correction of the form

$$E_u = \frac{U_{eff}}{2}[(N - N_0) - (N - N_0)^2], \quad (2)$$

where N is the local occupancy at the atomic site, $\lfloor N \rfloor = N_0$, and U_{eff} is a corrective parameter.

DFT+U functionals [37–40] have often been employed as a correction to local-MSIE. Much like Eq. (2), DFT+U-like functionals are comprised of linear and quadratic occupancy-dependent energy corrections. For example, Dudarev *et al.*'s 1998 Hubbard corrective functional [40] can be written as

$$E_u^{Dudarev} = \frac{U_{eff}}{2} \sum_{\sigma m} n_{mm}^{I\sigma} - \left(n_{mm}^{I\sigma}\right)^2. \quad (3)$$
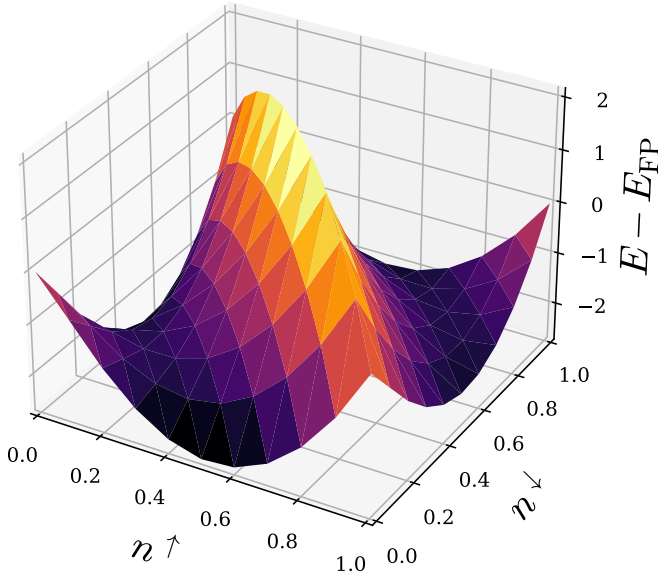
FIG. 1. Deviation of the total energy E in eV, of the He atom/ion for different values of spin-up ($n^\uparrow$) and spin-down ($n^\downarrow$) occupancy using the PBE exchange-correlation functional [3]. The PBE total energy is assumed to be exact at integer values of $n^\uparrow$ and $n^\downarrow$ for the He species. The exact energy from the flat plane condition is denoted as E_{FP}.

Unlike Eq. (2), here the corrections are given in terms of subspace occupancy matrix elements

$$n_{mm'}^{I\sigma} = \langle \phi_m^I | \hat{\rho}^\sigma | \phi_{m'}^I \rangle, \qquad (4)$$

where $\hat{\rho}^\sigma$ is the spin-σ Kohn-Sham density operator and $\{\phi_m\}$ are the set of atomically localized orbitals at atom I (the

atomic site index is often suppressed for clarity). Equation (3) is written in the basis of localized orbitals that diagonalize this subspace occupancy matrix. In the case where (i) the fractional occupancy at the atomic site is limited to the s-spin channel of one orbital ϕ_m, i.e., $n_{mm}^s = N - N_0$ and (ii) all other orbitals $\phi_{m'}$ are fully occupied or unoccupied, Dudarev's 1998 functional provides a perfect correction for local-MSIE.

Despite DFT+U's success in alleviating local-MSIE in this limiting case, here we stress two points. First, the DFT+U method was originally derived from the Hubbard model and it is merely fortuitous that it acts as a correction to local-MSIE. Second, the DFT+U method does not correct static correlation error and will therefore not satisfy the local flat plane condition.

In this Letter, we instead derive a DFT+U-type functional, disregarding entirely its connection with the Hubbard model and instead motivating its form entirely on the local analog of the flat plane condition. Such a functional should, for a single orbital subspace, satisfy the following four key conditions.

(1) Be a continuous function of the subspace electron count N and subspace magnetization M.

(2) Yield no correction at integer values of N and M. This is desirable because (semi-)local functionals are expected to yield accurate total energies in this case.

(3) Have a constant curvature of $-U^\sigma$ with respect to n^σ. This is desirable because (semi-)local functionals are expected to have a spurious curvature with respect to n^σ due to their deviation from the local flat plane condition.

(4) Have a constant curvature of J with respect to M. This is desirable because (semi-)local functionals are expected to have a spurious curvature with respect to M, again due to their deviation from the local flat plane condition.

The functional which satisfies these four key conditions is BLOR (Burgess-Linscott-O'Regan), given for each site by

$$E_{\mathrm{BLOR}} = \begin{cases} \dfrac{U^\uparrow + U^\downarrow}{4}\mathrm{Tr}[\hat{N} - \hat{N}^2] \;+\; \dfrac{J}{2}\mathrm{Tr}[\hat{M}^2 - \hat{N}^2] \;+ \dfrac{U^\uparrow - U^\downarrow}{4}\mathrm{Tr}[\hat{M} - \hat{N}\hat{M}], & \mathrm{Tr}[\hat{N}] \leqslant \mathrm{Tr}[\hat{P}]. \\[2mm] \underbrace{\dfrac{U^\uparrow + U^\downarrow}{4}\mathrm{Tr}[(\hat{N} - \hat{P}) - (\hat{N} - \hat{P})^2]}_{\text{Symmetric-MSIE term}} + \underbrace{\dfrac{J}{2}\mathrm{Tr}[\hat{M}^2 - (\hat{N} - 2\hat{P})^2]}_{\text{SCE term}} + \underbrace{\dfrac{U^\uparrow - U^\downarrow}{4}\mathrm{Tr}[\hat{M} - \hat{N}\hat{M}]}_{\text{Asymmetric-MSIE term}}, & \mathrm{Tr}[\hat{N}] > \mathrm{Tr}[\hat{P}]. \end{cases} \qquad (5)$$

Here $\hat{P}$ is the subspace projection operator $\hat{P} = \sum_m |\phi_m\rangle \langle \phi_m|$. The subspace occupancy and magnetization operators can be expressed in terms of the spin-resolved subspace occupancy operators $\hat{N} = \hat{n}^\uparrow + \hat{n}^\downarrow$ and $\hat{M} = \hat{n}^\uparrow - \hat{n}^\downarrow$, where $\hat{n}^\sigma = \hat{P}\hat{\rho}^\sigma \hat{P}$. The magnitude of the correction is controlled by three scalars: $U^\uparrow$, $U^\downarrow$, and J, which correspond, respectively, to the curvature with respect to $n^\uparrow$, $n^\downarrow$, and M. A full derivation of BLOR is given in S-I. One can show that conditions (1) to (4) are uniquely satisfied by BLOR (see S-II). The lower and upper versions of the functional have a similar form (the lower version of BLOR is the case where $\mathrm{Tr}[\hat{N}] \leqslant \mathrm{Tr}[\hat{P}]$).

The first term is referred to as the symmetric-MSIE term because, for a single orbital subspace, it yields zero correction at integer values of N and yields its maximum correction at $N = \frac{1}{2}, \frac{3}{2}$ as shown in the left panel of Fig. 2.

The second term is labeled as the SCE term because, for a single-orbital subspace, it yields zero correction when the subspace is maximally spin polarized and yields its maximum correction at $M = 0$ for a given value of N, as shown in the middle panel of Fig. 2.

The asymmetric-MSIE term will contribute to E_{BLOR} when an effective magnetic field acts on the subspace. In this case, we cannot assume that the curvatures $U^\uparrow$ and $U^\downarrow$ are equal in magnitude. This effective magnetic field may be caused by an external magnetic field acting on the isolated atomic site. More notably, in practical calculations, the target subspace will not be entirely isolated from its surrounding environment, such as the 3d subspace of face-centered cubic nickel. The 3d atomic subspace will experience an internal exchange-correlation magnetic field from the surrounding nickel atoms
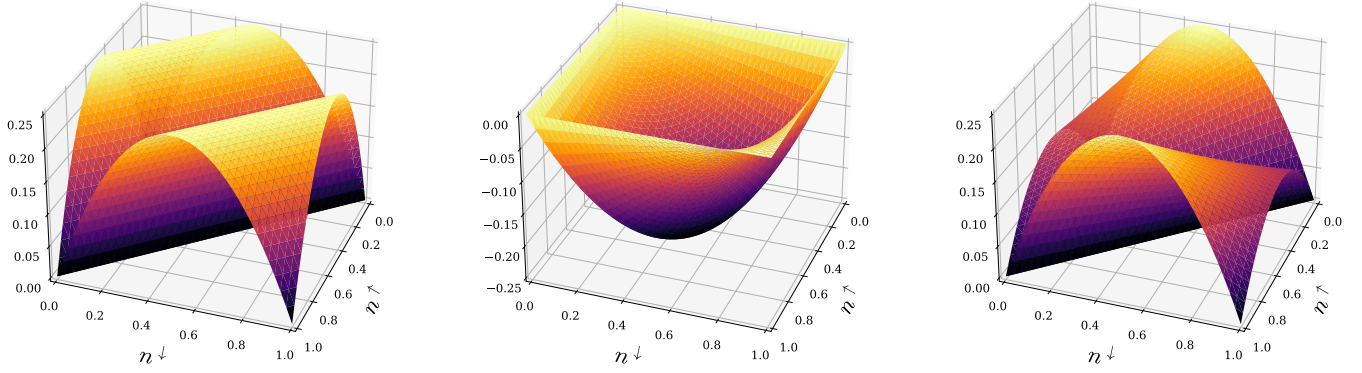
FIG. 2. The left panel presents the symmetric-MSIE term for an s-orbital subspace as a function of spin-up ($n^\uparrow$) and spin-down ($n^\downarrow$) subspace occupancy. The center panel presents the SCE term as a function of $n^\uparrow$ and $n^\downarrow$. The right panel presents the sum of the symmetric-MSIE and asymmetric-MSIE terms as a function of $n^\uparrow$ and $n^\downarrow$.

and hence we expect that $U^\uparrow \neq U^\downarrow$ for this site. The difference in magnitude is accounted for in the asymmetric-MSIE term. The combination of the symmetric- and asymmetric-MSIE terms is depicted in the right panel of Fig. 2, which, unlike

the left panel, shows a different curvature along the maximally spin-up polarized line compared to the maximally spin-down polarized line.

BLOR can also be expressed in terms of subspace occupancy matrix elements, for each site as

$$
E_{\text{BLOR}} = \begin{cases} \sum_{\sigma mm'} \dfrac{U^\sigma}{2} n^\sigma_{mm'} \delta_{mm'} - \dfrac{U^\sigma}{2} n^\sigma_{mm'} n^\sigma_{m'm} - \dfrac{U^\sigma + 2J}{2} n^\sigma_{mm'} n^{\bar\sigma}_{m'm}, & N \leqslant 2l+1. \\[3mm] \sum_{\sigma mm'} \left(U^\sigma + \dfrac{U^{\bar\sigma}}{2} + 2J \right) n^\sigma_{mm'} \delta_{mm'} - \dfrac{U^\sigma}{2} n^\sigma_{mm'} n^\sigma_{m'm} - \dfrac{U^\sigma + 2J}{2} n^\sigma_{mm'} n^{\bar\sigma}_{m'm} - \dfrac{U^\sigma + 2J}{2(2l+1)}, & N > 2l+1. \end{cases} \tag{6}
$$

In both cases, the summation runs over all terms on the right-hand side of Eq. (6).

BLOR has many similarities with existing functionals. For example, Himmetoglu *et al.*'s [41] DFT+U+J functional was recently modified by Bajaj *et al.* [42,43] to obtain jmDFT, a functional designed to correct for deviations from the global flat plane condition. However, jmDFT fails to satisfy conditions 3 and 4. Meanwhile, setting $U^\sigma = U_{\text{eff}}$, the first two terms of BLOR in the lower-half plane are equal to Dudarev *et al.*'s 1998 Hubbard functional. Furthermore, for non-spin-polarized systems we have that $U^\uparrow = U^\downarrow = U - J$ and the BLOR functional in the lower half plane simplifies to Moyni-han's DFT+U+J method which emulates self-consistency over the U and J parameters [44].

Before BLOR is applied to test systems, the corrective parameters U^σ and J must first be carefully chosen. Our aim is to use BLOR to explicitly enforce the E_{Hxc} flat plane condition on localized subspaces embedded within a material environment. It is worth noting that there is no exact flat plane condition on subspaces generally, but only in the limit of a fully isolated site, i.e., the fully dissociated/atomized limit. By explicitly enforcing the E_{Hxc} flat plane condition on localized states we implicitly assumed that all local curvature is spurious [35]. Accounting for overall charge and spin conservation, one can define the local curvature with respect to the spin-resolved subspace occupancy n^σ for a homonuclear,

diatomic system as

$$
U^\sigma = \frac{1}{2} \left(\frac{\partial^2 E_{\text{Hxc}}^{\text{approx}}}{\partial (n^\sigma)^2} \right)_{n^{\bar\sigma}}, \tag{7}
$$

and with respect to the subspace magnetization as

$$
J = -\frac{1}{2} \left(\frac{\partial^2 E_{\text{Hxc}}^{\text{approx}}}{\partial (M)^2} \right)_N, \tag{8}
$$

where N and M are the subspace electron count and magnetization and $E_{\text{Hxc}}^{\text{approx}}$ is the total Hxc energy using the approximate XC functional.

In this work, the corrective parameters U^σ and J were not calculated directly as second-order partial derivatives as defined by Eqs. (7) and (8). We chose instead to compute the corrective parameters from the Hxc potential. This can be achieved using the spin-resolved minimum tracking linear response methodology [44,45], which defines an effective subspace Hxc kernel as

$$
f^{\sigma\sigma'} = \frac{\partial}{\partial n^{\sigma'}} \left(\text{Tr}[\hat P]^{-1} \, \text{Tr}[\hat P \, \hat v^\sigma_{\text{Hxc}}] \right)_{n^{\bar\sigma'}}, \tag{9}
$$

where $\hat v^\sigma_{\text{Hxc}} = \delta E_{\text{Hxc}} / \delta \hat\rho^\sigma$ is the Hxc potential operator and we emphasize that one spin density is fixed while the other varies (E_{Hxc} is the Hxc energy of the system). Within this formalism the spin-resolved Hubbard parameters for BLOR can be set as

the diagonal elements of the Hxc kernel

$$U^\sigma = f^{\sigma\sigma}. \tag{10}$$

In Hubbard functionals not accepting a spin-indexed U, the spin-agnostic U parameter was evaluated by Linscott et al.'s simple 2×2 prescription

$$U = \tfrac{1}{4}(f^{\uparrow\uparrow} + f^{\uparrow\downarrow} + f^{\downarrow\uparrow} + f^{\downarrow\downarrow}), \tag{11}$$

which emulates the partial derivative with respect to the spin index. Analogously, the Hund's J parameter can be computed as

$$J = -\tfrac{1}{4}(f^{\uparrow\uparrow} - f^{\uparrow\downarrow} - f^{\downarrow\uparrow} + f^{\downarrow\downarrow}). \tag{12}$$

We note that by constructing J from the elements of the spin-resolved Hxc kernel, we sidestep the need to perform a constrained DFT calculation [as required by Eq. (8)]: the above equation for J obtains the same result via unconstrained linear-response calculations [45]. Sample linear-response graphs can be found in the Supplemental Material [46] (with sections and figures denoted as S), specifically Figs. S12 to S18. As shown in Supplemental Material section S-V, the Hubbard functionals were also tested using a variety of prescriptions for the U and J parameters. All further computational details can be found in S-VI while S-VII gives a practical scheme for implementing various corrective functionals including BLOR.

In Eqs. (5) and (6), BLOR is expressed in a generalized, from which readily allows its implementation for s, p, d, or f valence orbitals. However, in this Letter we explore BLOR's application solely to s-valence species, in which case there is no ambiguity as to whether the local flat plane condition should be enforced on the localized subspace as a whole or on each localized orbital in the subspace separately. The later of these two options was used to give BLOR in its current form, however, analysis of this choice through benchmarking with p and d valence species will be left to future work.

BLOR was first tested on s-block dimers, (namely, H_2, He_2^+, Li_2, and Be_2^+) with large internuclear separation lengths. It is assumed that, at these elongated bond lengths, the energy of the X_2 dimer is additive

$$E[X_2] = 2E[X]. \tag{13}$$

The subspace occupancies of the atomic species will be located at the vertices of the diamond, hence the bare Perdew-Burke-Ernzerhof (PBE) approximation [3] is expected to be reasonably accurate for $E[X]$. We thus assume that $2E_{PBE}[X]$ yields the exact total energy of our stretched X_2 species. This approximation benefits from cancellation of errors due to practical approximations including (very hard) pseudopotentials. The atomic subspaces of dissociated H_2 and Li_2 are approximately located along the $N = 1$ line of the diamond (the fold) and are thus dominated by local-SCE. The atomic subspaces of dissociated He_2^+ and Be_2^+ are approximately located along the edges of the diamond and are thus dominated by local-MSIE. These errors will result in the computed $E[X_2] \neq 2E[X]$ for the stretched X_2 species.

In Fig. 3 we present the relative errors in the total energies for H_2 at a bond length of $9a_0$ using different corrective functionals. PBE yields a significant relative error of 7.99%,
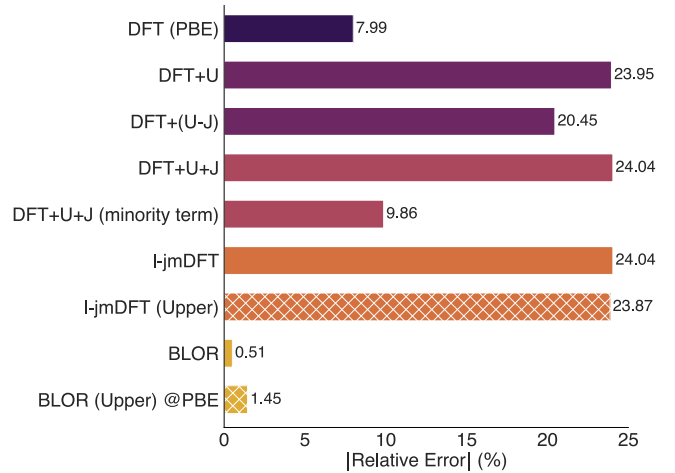

FIG. 3. Bar chart of the relative errors in the total energies of H_2 at a bond length of $9a_0$ using different corrective functionals [3,40–43,47], without spurious spin-symmetry breaking. The raw DFT calculations were performed with the PBE exchange correlation functional [3]. The DFT+U and DFT+($U-J$) relative errors were computed using Dudarev et al.'s 1998 functional with the effective Hubbard parameter (U_{eff}) set as U and $U - J$, respectively. Himmetoglu et al.'s DFT+U+J functional was employed both with and without the minority spin term. Both the lower and upper versions of l-jmDFT and BLOR are included in the bar chart. In the dissociated limit of H_2, each H atom will be singly occupied and hence the lower versions of BLOR and l-jmDFT are the relevant versions for dissociated H_2, despite the computed occupancy due to spillage being greater than one at the large but finite bond length of $9a_0$. The hashing on the bars of the upper versions of BLOR and l-jmDFT indicates the deliberate misapplication of these functionals. The BLOR (upper) corrective functional was evaluated on the PBE density, as discussed in the main text.

however, most of the corrective functionals significantly worsen the PBE result, yielding errors up to 24.04%. Use of BLOR in the lower half-plane yields a very low error of 0.510%. As shown in S-IV, BLOR yields even lower relative errors for dissociated He_2^+, Li_2, and Be_2^+.

In the bar chart our use of the jmDFT functional form is denoted as l-jmDFT (localized-jmDFT). The jmDFT functional was designed to correct for deviations from the global flat plane condition and was the main inspiration for the development of BLOR, which instead text focuses on the local flat plane condition. In this work, the jmDFT functional is implemented to correct for deviations from the local flat plane condition as opposed to the global equivalent. Furthermore, we use the simple 2×2 method to compute the U and J parameters for the jmDFT functional, which is not how the functional was intended to be applied. The poor performance of l-jmDFT is thus unsurprising.

Excluding the minority spin term, it is possible to reformulate the DFT+U and DFT+U+J functionals in terms of an MSIE-term $\text{Tr}[\hat{N} - \hat{N}^2]$ and a SCE-term $\text{Tr}[\hat{M}^2 - \hat{N}^2]$, with different linear combinations of U and J as prefactors. In the case of stretched H_2, the MSIE-term is negligible because the atomic occupancy is equal to 1 in the fully dissociated limit. Thus, the failure of the DFT+U and DFT+U+J functionals to predict the correct total energy can be attributed

FIG. 5. The decomposition of the total corrective energy associated with several functionals [40–43,47] into a symmetric-MSIE term, a SCE term, a minority-spin term, and an asymmetric-MSIE term. The exact corrective energy is that required to recover the correct dissociated-limit total energy.
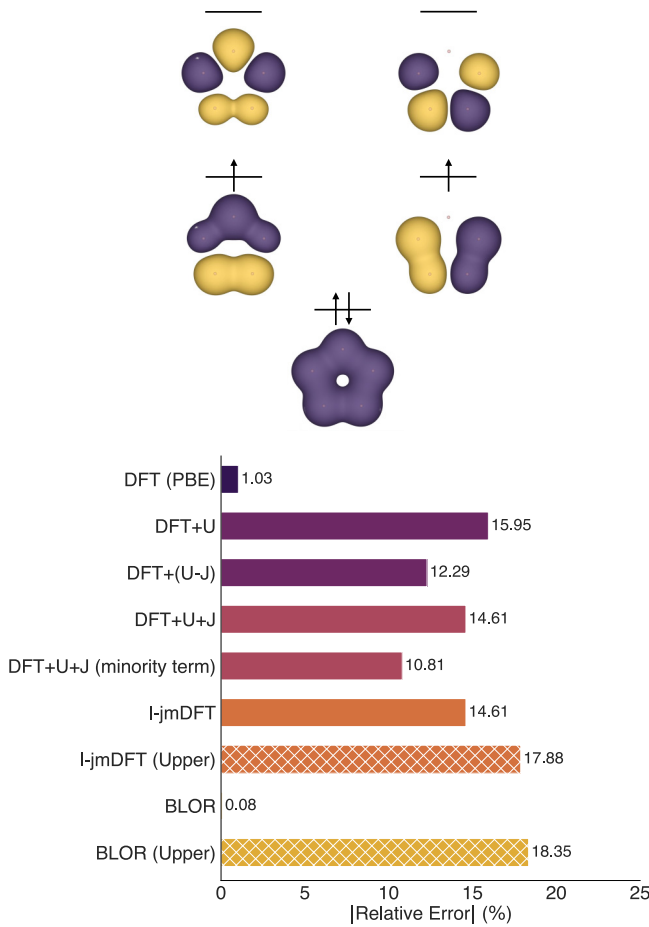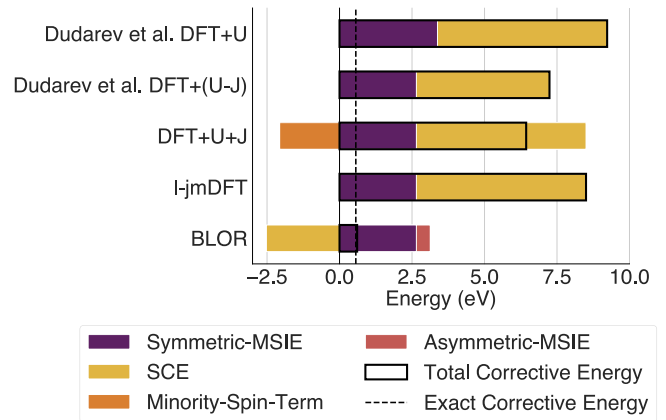

FIG. 4. The top panel displays isosurfaces of the five lowest spin up Kohn-Sham orbitals of the dissociated H_5^+ ring [48]. The bottom planel displays a bar chart of the relative errors in the total energy of dissociated H_5^+ at an internuclear separation of $8a_0$ using different corrective functionals [3,40–43,47], which are applied non-self-consistently on the extrapolated, symmetry-unbroken PBE spin-density. The atomic subspace occupancy is significantly less than 1 and will be equal to 0.8 at the dissociated limit, thus the lower versions of BLOR and l-jmDFT are the correct versions for this system.

correspondingly correct the KS potential; rectifying this issue will be left to future work.

The second system we tested BLOR on was a dissociated hydrogen ring system, which suffers from both local-MSIE and local-SCE (in a system where both local-MSIE and local-SCE are present, error cancellation may occur). Specifically, we look at the triplet spin state of this system, which provides a stringent test for the validity of the nascent asymmetric-MSIE correction term. Dissociated triplet H_5^+ is the smallest hydrogen ring system where (1) the subspaces are not located along the edge or fold of the diamond and (2) the system does not suffer from KS orbital degeneracy problems (where a degenerate pair of KS orbitals is occupied by a single KS particle). For dissociated H_5^+, bare PBE was found to yield a spurious symmetry-broken solution in what should be a five-fold symmetric spin-density. To stabilize the correct symmetry-unbroken solution, a potential of the form

$$\hat{v}^\sigma = G\hat{n}^{\bar{\sigma}} \qquad (14)$$

was applied to the atomic subspaces. The total PBE energy and spin-resolved subspace occupancies were then evaluated as functions of G and extrapolated to $G = 0$ to get the correct PBE energy and spin-resolved subspace occupancies. These occupancies were then used to obtain the total energy of the H_5^+ system evaluated on the extrapolated, symmetry-unbroken PBE spin-density for different corrective functionals including BLOR.

As shown in Fig. 4, bare PBE yields a very low relative error of 1.03% for the dissociated H_5^+ system. Application of any functional is found to worsen the bare PBE result, with the exception of BLOR, which yields a relative error of 0.08%. This extremely low error is investigated further in Fig. 5, where the total energy associated with several corrective functionals is decomposed into a symmetric-MSIE term, a SCE term, and an asymmetric-MSIE term. All corrective functionals shown yield similar positive energies for the symmetric-MSIE term. However, the corrective functionals all yield large *positive* SCE terms with the exception of

to the incorrect SCE-term prefactor of $-U/4$ in both cases. Indeed, computing the total energy of H_2 at a $9a_0$ bond length with both symmetric-MSIE and asymmetric-MSIE prefactors being equal to 0, but with the correct SCE prefactor of $J/2$, yields a relative error of 0.81%.

Several of the corrective functionals (including BLOR) were found, at least on the basis of molecular orbital theory analysis, to yield the incorrect ordering of the Kohn-Sham (KS) orbitals upon self-consistent application of the corrective functional. Whenever this occurred, the corrective functional was applied non-self-consistently, i.e., the total energy was evaluated on the PBE density, hence we have BLOR@PBE. For all corrective functionals where no KS orbital reordering occurs, the total energy was evaluated both self-consistently and non-self-consistently and the difference between the two was found to be negligible. This demonstrates that BLOR yields correct total energies but fails to

BLOR. A positive SCE term leads to a significant overestimation of the total corrective energy.

In conclusion, our derived corrective functional BLOR yielded relative energetic errors below 0.6% across all five dissociated s-block species. This performance was unmatched by any of the other DFT+U-type functionals tested. However, the BLOR corrective functional yielded a spurious reordering of the KS orbitals for He_2^+ and Be_2^+, as judged from molecular orbital theory considerations. This problem was bypassed for these systems by evaluating the BLOR energy at the PBE density (BLOR@PBE). Most notably, our DFT+U-type corrective functional was derived entirely from first principles, based on the flat plane behavior of exact quantum mechanics.

It thereby lifts the assumptions required when deriving such functionals from the Hubbard model.

[1] P. Hohenberg and W. Kohn, Inhomogeneous Electron Gas, Phys. Rev. **136**, B864 (1964).

[2] S. H. Vosko, L. Wilk, and M. Nusair, Accurate spin-dependent electron liquid correlation energies for local spin density calculations: A critical analysis, Can. J. Phys. **58**, 1200 (1980).

[3] J. P. Perdew, K. Burke, and M. Ernzerhof, Generalized Gradient Approximation Made Simple, Phys. Rev. Lett. **77**, 3865 (1996).

[4] J. P. Perdew, A. Ruzsinszky, G. I. Csonka, O. A. Vydrov, G. E. Scuseria, L. A. Constantin, X. Zhou, and K. Burke, Restoring the Density-Gradient Expansion for Exchange in Solids and Surfaces, Phys. Rev. Lett. **100**, 136406 (2008).

[5] A. D. Becke, Density-functional exchange-energy approximation with correct asymptotic behavior, Phys. Rev. A **38**, 3098 (1988).

[6] C. Lee, W. Yang, and R. G. Parr, Development of the Colle-Salvetti correlation-energy formula into a functional of the electron density, Phys. Rev. B **37**, 785 (1988).

[7] A. D. Becke, Density-functional thermochemistry. III. The role of exact exchange, J. Chem. Phys. **98**, 5648 (1993).

[8] J. Heyd, G. E. Scuseria, and M. Ernzerhof, Hybrid functionals based on a screened Coulomb potential, J. Chem. Phys. **118**, 8207 (2003).

[9] J. Sun, A. Ruzsinszky, and J. P. Perdew, Strongly Constrained and Appropriately Normed Semilocal Density Functional, Phys. Rev. Lett. **115**, 036402 (2015).

[10] J. Tao, J. P. Perdew, V. N. Staroverov, and G. E. Scuseria, Climbing the Density Functional Ladder: Nonempirical Meta–Generalized Gradient Approximation Designed for Molecules and Solids, Phys. Rev. Lett. **91**, 146401 (2003).

[11] N. Mardirossian and M. Head-Gordon, ωB97M-V: A combinatorially optimized, range-separated hybrid, meta-GGA density functional with VV10 nonlocal correlation, J. Chem. Phys. **144**, 214110 (2016).

[12] R. L. A. Haiduke and R. J. Bartlett, Non-empirical exchange-correlation parameterizations based on exact conditions from correlated orbital theory, J. Chem. Phys. **148**, 184106 (2018).

[13] Z. Lin and T. Van Voorhis, Triplet tuning: A novel family of non-empirical exchange-correlation functionals, J. Chem. Theory Comput. **15**, 1226 (2019).

[14] M. de Jong, W. Chen, T. Angsten, A. Jain, R. Notestine, A. Gamst, M. Sluiter, C. Krishna Ande, S. van der Zwaag, J. J. Plata, C. Toher, S. Curtarolo, G. Ceder, K. A. Persson, and M. Asta, Charting the complete elastic properties of inorganic crystalline compounds, Sci Data **2**, 150009 (2015).

[15] M. Zilka, D. V. Dudenko, C. E. Hughes, P. A. Williams, S. Sturniolo, W. T. Franks, C. J. Pickard, J. R. Yates, K. D. M. Harris, and S. P. Brown, Ab initio random structure searching of organic molecular solids: Assessment and validation against experimental data, Phys. Chem. Chem. Phys. **19**, 25949 (2017).

[16] A. Ruzsinszky, J. P. Perdew, G. I. Csonka, O. A. Vydrov, and G. E. Scuseria, Spurious fractional charge on dissociated atoms: Pervasive and resilient self-interaction error of common density functionals, J. Chem. Phys. **125**, 194112 (2006).

[17] A. D. Dutoi and M. Head-Gordon, Self-interaction error of local density functionals for alkali– halide dissociation, Chem. Phys. Lett. **422**, 230 (2006).

[18] J. Nafziger and A. Wasserman, Fragment-based treatment of delocalization and static correlation errors in density-functional theory, J. Chem. Phys. **143**, 234105 (2015).

[19] J. P. Perdew, Density functional theory and the band gap problem, Int. J. Quantum Chem. **28**, 497 (1985).

[20] P. Borlido, T. Aull, A. W. Huran, F. Tran, M. A. L. Marques, and S. Botti, Large-Scale Benchmark of Exchange–Correlation Functionals for the Determination of Electronic Band Gaps of Solids, J. Chem. Theory Comput. **15**, 5069 (2019).

[21] A. J. Cohen, P. Mori-Sánchez, and W. Yang, Fractional charge perspective on the band gap in density-functional theory, Phys. Rev. B **77**, 115123 (2008).

[22] T. Zhu and S.-P. Gao, The Stability, Electronic Structure, and Optical Property of TiO_2 Polymorphs, J. Phys. Chem. C **118**, 11385 (2014).

[23] A. Schrön, C. Rödl, and F. Bechstedt, Energetic stability and magnetic properties of MnO in the rocksalt, wurtzite, and zinc-blende structures: Influence of exchange and correlation, Phys. Rev. B **82**, 165109 (2010).

[24] G. Sai Gautam and E. A. Carter, Evaluating transition metal oxides within DFT-SCAN and SCAN+U frameworks for solar thermochemical applications, Phys. Rev. Mater. **2**, 095401 (2018).

[25] J. P. Perdew, R. G. Parr, M. Levy, and J. L. Balduz, Density-Functional Theory for Fractional Particle Number: Derivative Discontinuities of the Energy, Phys. Rev. Lett. **49**, 1691 (1982).

[26] W. Yang, Y. Zhang, and P. W. Ayers, Degenerate Ground States and a Fractional Number of Electrons in Density and Reduced Density Matrix Functional Theory, Phys. Rev. Lett. **84**, 5172 (2000).

[27] A. J. Cohen, P. Mori-Sánchez, and W. Yang, Fractional spins and static correlation error in density functional theory, J. Chem. Phys. **129**, 121104 (2008).

[28] P. Mori-Sánchez, A. J. Cohen, and W. Yang, Many-electron self-interaction error in approximate density functionals, J. Chem. Phys. **125**, 201102 (2006).

[29] T. J. Callow, B. Pearce, and N. I. Gidopoulos, Density functionals with spin-density accuracy for open shells, J. Chem. Phys. **156**, 111101 (2022).

[30] P. Mori-Sánchez, A. J. Cohen, and W. Yang, Discontinuous Nature of the Exchange-Correlation Functional in Strongly Correlated Systems, Phys. Rev. Lett. **102**, 066403 (2009).

[31] X. D. Yang, A. H. G. Patel, R. A. Miranda-Quintana, F. Heidar-Zadeh, C. E. González-Espinoza, and P. W. Ayers, Communication: Two types of flat-planes conditions in density functional theory, J. Chem. Phys. **145**, 031102 (2016).

[32] P. W. Ayers, The dependence on and continuity of the energy and other molecular properties with respect to the number of electrons, J Math Chem **43**, 285 (2008).

[33] R. Cuevas-Saavedra, D. Chakraborty, S. Rabi, C. Cárdenas, and P. W. Ayers, Symmetric Nonlocal Weighted Density Approximations from the Exchange-Correlation Hole of the Uniform Electron Gas, J. Chem. Theory Comput. **8**, 4081 (2012).

[34] P. Mori-Sánchez and A. J. Cohen, The derivative discontinuity of the exchange– correlation functional, Phys. Chem. Chem. Phys. **16**, 14378 (2014).

[35] Q. Zhao, E. I. Ioannidis, and H. J. Kulik, Global and local curvature in density functional theory, J. Chem. Phys. **145**, 054109 (2016).

[36] D. Hait and M. Head-Gordon, Delocalization Errors in Density Functional Theory Are Essentially Quadratic in Fractional Occupation Number, J. Phys. Chem. Lett. **9**, 6280 (2018).

[37] V. I. Anisimov, J. Zaanen, and O. K. Andersen, Band theory and Mott insulators: Hubbard U instead of Stoner I, Phys. Rev. B **44**, 943 (1991).

[38] V. I. Anisimov, I. V. Solovyev, M. A. Korotin, M. T. Czyżyk, and G. A. Sawatzky, Density-functional theory and NiO photoemission spectra, Phys. Rev. B **48**, 16929 (1993).

[39] A. I. Liechtenstein, V. I. Anisimov, and J. Zaanen, Density-functional theory and strong interactions: Orbital ordering in Mott-Hubbard insulators, Phys. Rev. B **52**, R5467(R) (1995).

[40] S. L. Dudarev, G. A. Botton, S. Y. Savrasov, C. J. Humphreys, and A. P. Sutton, Electron-energy-loss spectra and the structural stability of nickel oxide: An LSDA+U study, Phys. Rev. B **57**, 1505 (1998).

[41] B. Himmetoglu, R. M. Wentzcovitch, and M. Cococcioni, First-principles study of electronic and structural properties of CuO, Phys. Rev. B **84**, 115108 (2011).

[42] A. Bajaj, J. P. Janet, and H. J. Kulik, Communication: Recovering the flat-plane condition in electronic structure theory at semi-local DFT cost, J. Chem. Phys. **147**, 191101 (2017).

[43] A. Bajaj, F. Liu, and H. J. Kulik, Non-empirical, low-cost recovery of exact conditions with model-Hamiltonian inspired expressions in jmDFT, J. Chem. Phys. **150**, 154115 (2019).

[44] G. Moynihan, A self-contained ground-state approach for the correction of self-interaction error in approximate density-functional theory, Ph.D. thesis, School of Physics, Trinity College Dublin, 2018.

[45] E. B. Linscott, D. J. Cole, M. C. Payne, and D. D. O'Regan, Role of spin in the calculation of Hubbard U and Hund's J parameters from first principles, Phys. Rev. B **98**, 235157 (2018).

[46] See Supplemental Material at http://link.aps.org/supplemental/10.1103/PhysRevB.107.L121115 for further references [49–61], including S-I the derivation of the BLOR functional; S-II a proof of the uniqueness of that functional; S-III a suggested method for immediate use of the BLOR functional; S-IV a dissociation energy error analysis on the five systems and 15 functionals tested; S-V a representative subset of the latter repeated using three alternative methods for computing U and J parameters; S-VI the computational details of the study; S-VII guidance on how the functionals tested may be invoked without software modification; and S-VIII a sample demonstration of the linear response calculations performed to compute U and J.

[47] S. L. Dudarev, P. Liu, D. A. Andersson, C. R. Stanek, T. Ozaki, and C. Franchini, Parametrization of LSDA+U for noncollinear magnetic configurations: Multipolar magnetism in UO_2, Phys. Rev. Mater. **3**, 083802 (2019).

[48] K. Momma and F. Izumi, VESTA A three-dimensional visualization system for electronic and structural analysis, J. Appl. Cryst. **41**, 653 (2008).

[49] M. Cococcioni and S. de Gironcoli, Linear response approach to the calculation of the effective interaction parameters in the LDA+U method, Phys. Rev. B **71**, 035105 (2005).

[50] M. T. Czyżyk and G. A. Sawatzky, Local-density functional and on-site correlations: The electronic structure of La_2CuO_4 and $LaCuO_3$, Phys. Rev. B **49**, 14211 (1994).

[51] E. R. Ylvisaker, W. E. Pickett, and K. Koepernik, Anisotropy and magnetism in the LSDA+U method, Phys. Rev. B **79**, 035103 (2009).

[52] M. Shishkin and H. Sato, Challenges in computational evaluation of redox and magnetic properties of Fe-based sulfate cathode materials of Li- and Na-ion batteries, J. Phys.: Condens. Matter **29**, 215701 (2017).

[53] M. Shishkin and H. Sato, in Dudarev's formulation with corrected interactions between the electrons with opposite spins: The form of Hamiltonian, calculation of forces, and bandgap adjustments, J. Chem. Phys. **151**, 024102 (2019).

[54] D.-K. Seo, Self-interaction correction in the LDA+U method, Phys. Rev. B **76**, 033102 (2007).

[55] J. C. A. Prentice, J. Aarons, J. C. Womack, A. E. A. Allen, L. Andrinopoulos, L. Anton, R. A. Bell, A. Bhandari, G. A. Bramley, R. J. Charlton, R. J. Clements, D. J. Cole, G. Constantinescu, F. Corsetti, S. M.-M. Dubois, K. K. B. Duff, J. M. Escartín, A. Greco, Q. Hill, L. P. Lee *et al.*, The ONETEP linear-scaling density functional theory program, J. Chem. Phys. **152**, 174111 (2020).

[56] C.-K. Skylaris, P. D. Haynes, A. A. Mostofi, and M. C. Payne, Introducing ONETEP: Linear-scaling density functional simulations on parallel computers, J. Chem. Phys. **122**, 084119 (2005).

[57] C.-K. Skylaris, A. A. Mostofi, P. D. Haynes, O. Diéguez, and M. C. Payne, Nonorthogonal generalized Wannier function pseudopotential plane-wave method, Phys. Rev. B **66**, 035119 (2002).

[58] D. D. O'Regan, N. D. M. Hine, M. C. Payne, and A. A. Mostofi, Linear-scaling DFT+U with full local orbital optimization, Phys. Rev. B **85**, 085107 (2012).

[59] G. J. Martyna and M. E. Tuckerman, A reciprocal space based method for treating long range interactions in ab initio and force-field-based calculations in clusters, J. Chem. Phys. **110**, 2810 (1999).

[60] OPIUM: The optimized pseudopotential interface unification module, https://opium.sourceforge.net.

[61] O. K. Orhan and D. D. O'Regan, First-principles Hubbard U and Hund's J corrected approximate density functional theory predicts an accurate fundamental gap in rutile and anatase TiO$_2$, Phys. Rev. B **101**, 245137 (2020).